Chapter 6

Behavior of Reinforced Soil Wall Built with Fabrics

Mario Riccio and Mauricio Ehrlich

Additional information is available at the end of the chapter

http://dx.doi.org/10.5772/intechopen.79239

Abstract

This chapter presents an example of use of fabrics in geotechnical engineering construction. Some aspects related to design, construction, and the performance of a 4.2-m-high-reinforced soil wall, located in Brazil, is presented. In this wall, geogrid (fabric reinforcement) was used as reinforcement, and the backfill was a fine-grained residual tropical soil. The wall was monitored during its construction (2 months); load in the reinforcements, vertical and horizontal displacements of the reinforced soil mass, and efforts on block-face were measured. The monitoring of the wall was done by means of load cells for the reinforcements and block-face, and also includes settlement plates, total pressure cells, inclinometers, and topographical marks. The results provided by the instruments showed good performance of the wall. Measurements and calculated tension in the reinforcements were compared, and good prediction capability of the used analytical method was demonstrated. The measured tensile load in the reinforcements was lower than the admissible load of the geogrids used in the wall. Measurements also indicate that the block-face was able to support part of the load that would be carried by the reinforcements.

Keywords: fabrics, reinforced soil wall, monitoring, analytical method

1. Introduction

Reinforced soil walls (RSW) are retaining structures composed by facing, compacted backfill and usually geosynthetic reinforcements. Compacted soils have good strength in terms of compression solicitation, but they have a very low tensile strength. Thus, similar to the reinforced concrete, the use of fabrics as reinforcement is intended to provide enough tension resistance to the composite material. RSW structures can be built with a wide variety of fabrics (geosynthetics). Those fabrics are specially developed and have different applications in geotechnical engineering. **Figure 1** shows some examples of geosynthetics used in RSW construction as reinforcement.

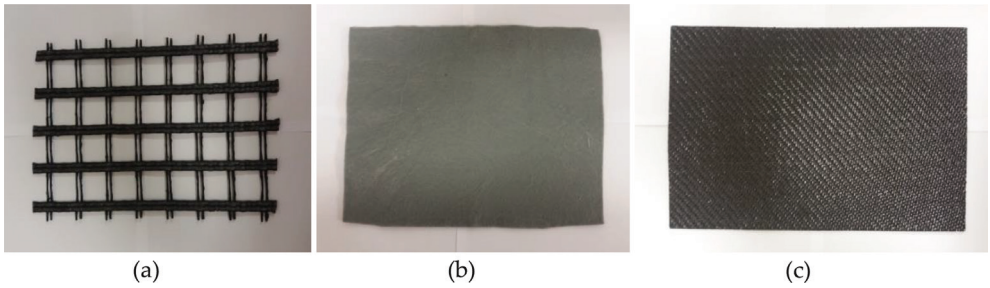

Figure 1. Examples of geosynthetics used for RSW construction as reinforcement: (a) geogrid; (b) nonwoven geotextile; (c) woven geotextile.

The backfill used for reinforced soil wall construction could be purely sands or even soils that contain high percentage of fines. In Brazil, due to the abundance of residual fine-grained soils, it is a common practice to build RSW using this kind of soil. This kind of soils, in spite of its high percentage of fines, has high strength resistance, presents good workability, and achieves a proper density during compaction. **Figure 2** shows the basic concept of RSW; the geosynthetics link the active zone (the unstable zone) to the resistant zone. Design should provide enough reinforcements in order to guarantee no failure or pullout of reinforcements from the resistant zone. Both zones liked together works like a block that may be considered as a conventional retaining wall that provides the stabilization of the nearby nonreinforced soil mass. The mobilized load along the reinforcements is variable, and the location of the points of maximum tension defines the potential failure surface that separates the active and passive zones. **Figure 2** also indicates the shape of the potential failure surface that varies with the stiffness of reinforcements.

The design of an RSW comprises basically two verifications: (a) external stability that is basically the same concept used for the conventional retaining walls, i.e., stability analyses for sliding and

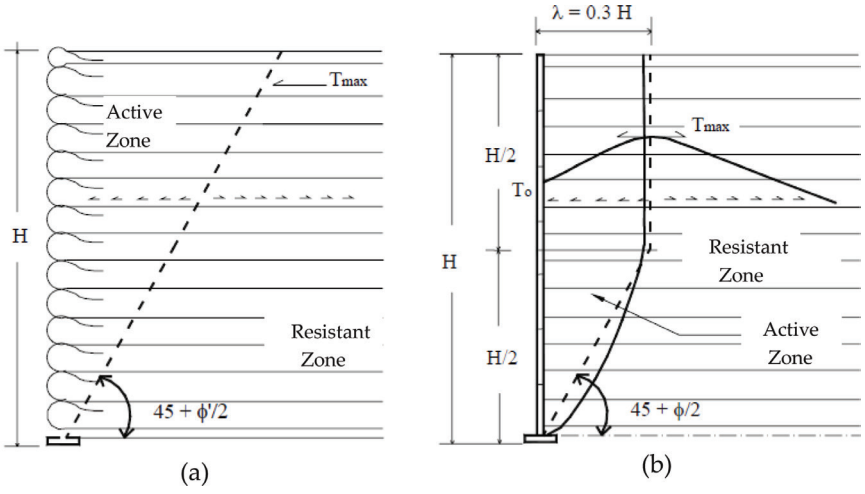

Figure 2. Basic concept of RSW and the potential failure surface: for extensible (a) and rigid (b) reinforcements.

overturning, bearing capacity and general failure and (b) internal stability. The internal stability consists in the comparison of the mobilized load in the reinforcements (geosynthetic) with the tension strength of those ones. There are some methods to evaluate the mobilized load in the reinforcements, such as [1–5]. Through case studies, field instrumentation, physical and numerical modeling [6–11] have been demonstrated that among these methods the more suitable are the ones proposed in [4, 5]. These methods explicitly consider soil and reinforcement properties, the effect of compaction operation, and the relative stiffness between soil and reinforcement. The method described in [5] is based on the one developed by Ehrlich and Mitchell [4]; this method uses simple equations and may take in the calculation facing inclination into consideration.

Figure 3 shows different concepts of facing elements. In the RSW structures, facing has a secondary function, and it is used to avoid erosion and localized soil failure near to the face, besides providing suitable visual appearance. Precast concrete block-face is usually used in RSWs with geogrid reinforcements (**Figure 3c**). Precast concrete block-face is also used in the case of RSW with geosynthetic wrap-around facing (**Figure 3a**). This block-facing is applied after the end of the wall construction, and it is needed to protect geosynthetics from degradation due to exposure to ultraviolet rays and vandalism. Depending on its rigidity, the face may be capable to absorb part of the tension that would be supported by the reinforcements. Nevertheless, the design of internal stability is usually done without consideration of the facing contribution to the global stability, if it exists. Note that this approach is by the side of safety [6]. Moreover, enough drainage must be employed in order to guarantee no positive

Figure 3. Typical facing elements: (a) geosynthetic wrap-around facing before protection application (courtesy: Ober geosynthetics); (b) precast-concrete panels (courtesy: Reinforced Earth Company); (c) precast-concrete blocks facing; and (d) steel mesh facing filled with stones (courtesy: Paulo Brugger).

pore-pressures inside the reinforced soil mass. The drainage system is often composed by a vertical layer of gravel behind the face and a horizontal layer at the RSW bottom.

2. The São Jose dos Campos RSW

This section describes and shows monitoring results of an RSW built in the year of 2006, as a part of a road construction in the city of Sao Jose dos Campos, state of Sao Paulo, Brazil [6]. This RSW has 4.2 m height, segmental concrete blocks composing the face, and geogrid as reinforcements and tropical fine-grained lateritic soil as backfill. In the field, the soil compaction was done through a heavy vibratory roller drum Dynapac CA250PD. Other previous studies have also ensured good mechanical behavior of RSWs where fine-grained soil was used as backfill [12–18]. The wall under consideration was extensively instrumented during 2 months (constructive period) to verify its overall performance. The instrumentation consisted of load cells for measurement of the mobilized loads in the reinforcements and block-face, settlement plates, total pressure cells, inclinometers, and topographical marks. The main results obtained are presented and discussed in this chapter. The instrumentation indicates good mechanical performance of the RSW. The wall under analysis has not indicated any structural problems or excessive deformations. In Section 3, some design considerations and comparison of measured load in the reinforcements and predictions are shown.

2.1. Overall characteristics of the Sao Jose dos Campos RWS

In the wall construction, two residual soils were used as backfill, both with high percentage of fines. The yellow sandy clay (soil A) was used from the top of the wall to the 3.2 m depth, and red sandy clay, from 3.2 m depth to the bottom of the wall. In **Table 1**, the grain-size distribution and Atterberg limits (liquid limit, w_L, and plasticity index, PI) of those soils are presented. Using the Unified Soil Classification System, both soils were classified as CL (low-plastic clays).

Those backfill soils were tested in laboratory by means of plane strain tests. The plane strain condition is representative of typical wall behavior where the longitudinal length of the wall is much greater than its height. Under these conditions, it is a reasonable assumption the consideration of the absence of longitudinal deformations. The soil specimens used on tests were compacted statically with the same unit weight (γ) and water content (w) verified in the field. In **Table 2**, the results of those tests are shown; where ϕ is the friction angle of the soil (total stress envelope); c is the cohesion of the soil (total stress envelope); n, k (for loading),

Soil	≤2 μm (%)	≤20 μm (%)	≤2 mm (%)	w_L (%)	PI (%)
A	42	49	99	38	22
B	42	47	99	49	29

Table 1. Soil grain size distribution and Atterberg limits.

Soil	γ (kN/m³)	w (%)	ϕ (°)	c (kPa)	n	k	k_u	Rf
A	16.7	20	36	60	0.47	392	588	0.86
B	16.7	20	38	50	0.36	566	849	0.95

Table 2. Results of plane strain tests performed on the backfill soils.

k_u (for unloading), and R_f are hyperbolic parameters obtained from the triaxial tests according to the procedure followed in [19]. In the absence of plane strain or triaxial tests, the values of n and k can be selected using the suggestion from [20]. The value of k_u can be considered as 1.5 k, and R_f equals to 0.90 as typical values.

Two different PET geogrids were used in this RSW as reinforcements. One was placed in the reinforcement layers 1–3 (bottom to top) and the other in the layers 4–7. In **Table 3**, the characteristics of those fabrics are shown. In **Table 4**, the characteristics of blocks used as facing are also presented. The blocks were filled with crushed stones, in order to increase the pullout resistance of the geogrid-blocks interface and guarantee drainage at the face.

2.2. Instrumentation

Figure 4 shows a general view of the wall just after the end of construction. In **Figures 5** and **6**, are shown a cross section and plan view of the wall with the location of the instruments used for monitoring, respectively. The wall has seven layers of reinforcements with 3 m length each. Four of those layers were instrumented, i.e., reinforcement layers 1, 4, 5, and 6 (see **Figure 5**).

Reinforcement layers	1–3	4–7
Ultimate longitudinal tensile strength (kN/m)	55	35
Ultimate transverse tensile strength (kN/m)	30	20
Elongation at rupture (%)	12.5	12.5
Weight (gf/m²)	360	210
Opening size (mm)	20 × 30	20 × 20
Stiffness modulus, J (kN/m) at 5% strain	400	260

Table 3. Physical and mechanical properties of the fabrics (geosynthetic).

Dimensions (m)	0.2 height, 0.40 long, 0.40 wide
Block weight (kgf)	29
Block with*crushed stone (kgf)	40–50
Compressive strength (MPa)	6–12

Table 4. Characteristics of concrete block used as facing.

Figure 4. General view of the RSW just after construction.

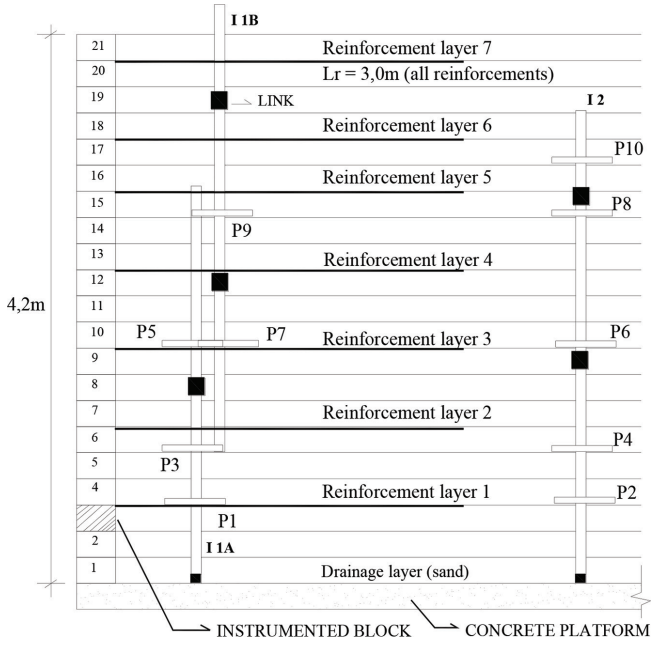

Figure 5. Cross section of instrumented wall: P is settlement plate and I is inclinometer, [6].

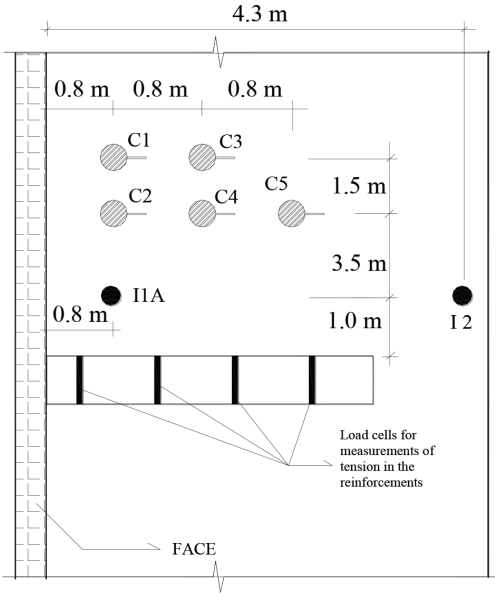

Figure 6. Location of the instruments in the first layer of reinforcement at 3.6 m depth, [6].

Inclinometers (I1A, I1B, and I2) and magnetic settlement plates (P1–P10) were used to measure lateral and vertical movements, respectively.

Topographical measurements were used for monitoring external horizontal displacements at face (topographic marks were located between the blocks 5 and 6 and between the blocks 13 and 14).

Figure 5 also indicates that the wall foundation is composed by a piled slab (concrete platform), due to the presence of soft soil beneath it. **Figure 6** shows the position of the inclinometers (I1A and I2), the load cells used for monitor the reinforcement load, and the total stress cells (C1–C5), located in the first layer of reinforcement at 3.6 m depth. Four load cells were positioned along the reinforcement (see **Figure 7**).

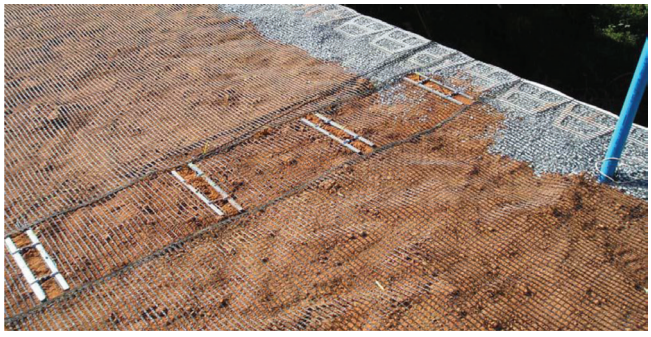

Figure 7. Load cells positioned along the reinforcement [21].

A special device was used for monitoring vertical and horizontal forces at the toe of the bock-face. A bipartite metallic block replaced one of the concrete-blocks that compose the facing (**Figure 8**). Six load cells were used inside this metallic block, four for vertical and two for horizontal load measurement.

Additional details of the instruments used for monitor load in the reinforcements (geogrid) and at the block-face could be found in [21].

2.3. Monitoring results

2.3.1. Tension on reinforcements

Figure 9 shows measured loads in the reinforcement layers at the end of construction (layers 1, 4, 5, and 6, see **Figure 5**). The maximum load recorded was verified in the reinforcement layer 5, and was equal to 7.1 kN/m. Note that the ultimate strength of the geogrid used at the layer 5 was equal to 35 kN/m (**Table 3**). At this layer, the point of maximum tensile load (T_{max}) in the reinforcement at this layer was located 1 m far from face. Notice that considering all layers, the position of the T_{max} does not exhibit a well-defined pattern with respect to the distance from face. This random behavior may be related to the difference of placement of the geogrid and the backfill compaction layers in the field.

2.3.2. Loads at the toe of the wall facing

In **Figure 10**, are shown vertical and horizontal loads measured in the instrumented block located at the toe of the block-face during wall construction. The instrumented metallic block is located in the third block-layer and is monitored by six load cells (see **Figures 5** and **8**).

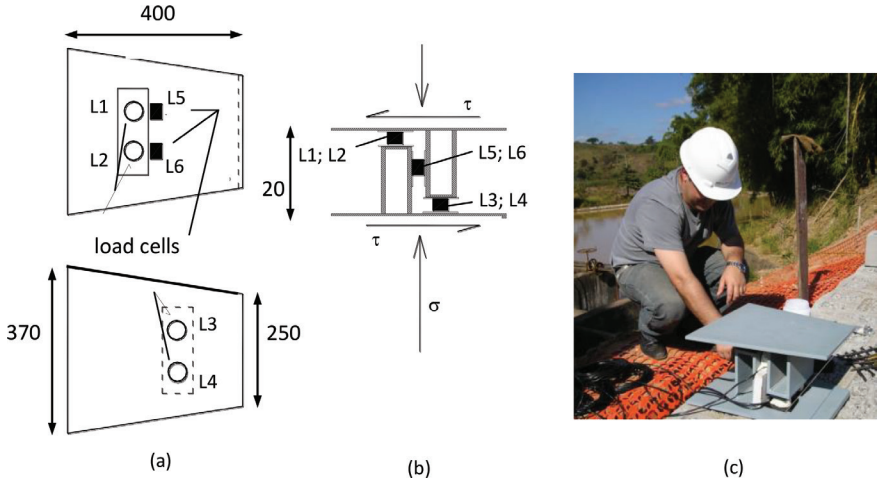

Figure 8. The metallic block used to measure load next to the toe of block-facing: (a) plan view, (b) section view, and (c) block positioned in the field; dimensions in millimeters [6].

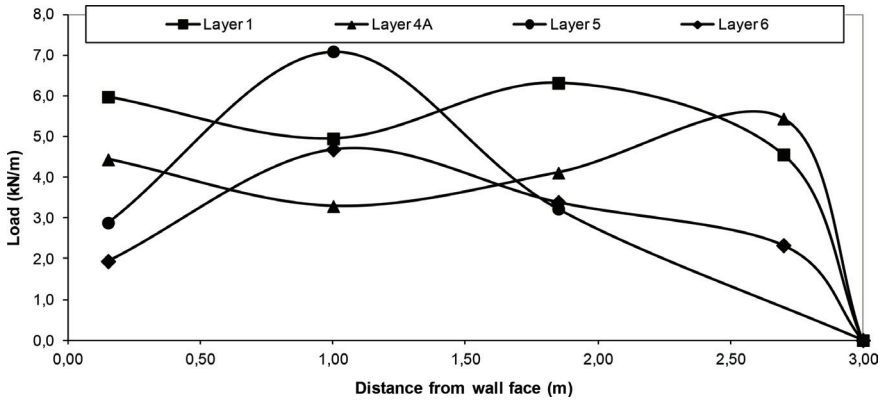

Figure 9. Load in reinforcements measured at the end of construction [6].

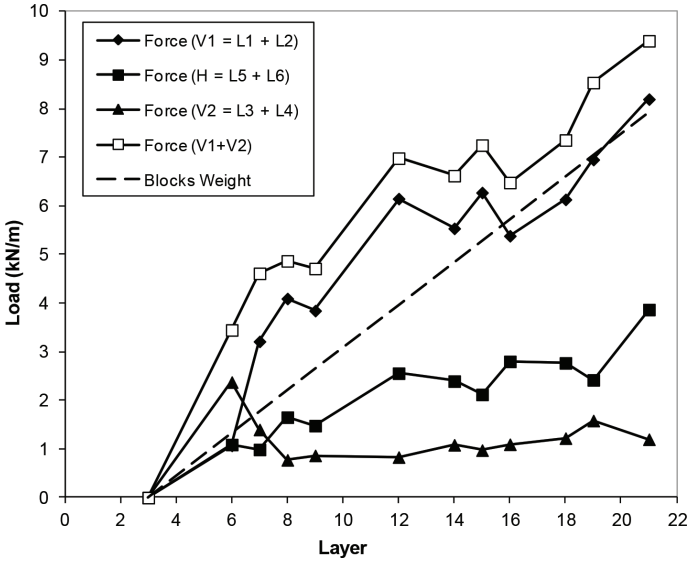

Figure 10. Vertical and horizontal loads measured in the instrumented block during the wall construction [6].

The front (L1 and L2) and rear (L3 and L4) load cells measure the vertical loads acting in the front (V1) and rear (V2) of the block. The load cells (L5 and L6) measured the horizontal load (H) acting in the block. Note that, in **Figure 10**, the front vertical load (V1 = L1 + L2) is often higher that the rear vertical load (V2 = L3 + L4). This behavior is related to the eccentricity of the resultant load due to the self-weight and lateral earth pressure at the interface with the reinforced soil mass that led to an overturn tendency at the block-facing. The dashed line represents the self-weight of the blocks filled with crushed stone, assuming vertical arrangement of the blocks. Notice that the total measured vertical load (V1 + V2) was always higher than

the self-weight of the blocks; this increase of vertical load is due to the mobilized friction at the interface of the block-face and backfill. The measured horizontal load at the toe block-face (H) is related to the restrain to the lateral movement at base of the blocks (fix-base condition), as discussed in [22]. Note that in the RSW under analysis, the first block-layer is tied to the concrete slab (see **Figure 2**). At free-base condition, no mobilization of horizontal load at the block-facing would be expected [22–24].

2.3.3. Vertical stresses at the bottom of the wall

Figure 11 presents the vertical stress measured by total stress cells (C2–C5, see **Figure 6**) and calculated values using the Meyerhof approach [25] for the first layer of reinforcement (3.6 m depth) at the end of construction. The Meyerhof approach [25] accounts for the eccentricity of the resultant due to the self-weight and the earth pressure exerted by the nonreinforced zone in the wall. The vertical stress provided by Meyerhof [25] is slightly higher than the vertical stress due the self-weight of backfill without any external load. This behavior is due the earth pressure caused by soil behind the reinforced zone. The study carried out by Riccio et al. [6] presents a more deep discussion about this behavior.

2.3.4. Horizontal displacements

Figure 12 shows the horizontal displacements measured at the end of wall construction by means of inclinometers (I1A, I1B, and I2; **Figure 5**) and by topographic readings at the end of construction. Significant movements were measured in I1A e I1B near to the face (~60 mm). Topographic readings in the facing at heights of 1.60 and 2.60 m unveil lateral displacements equal to 4 and 22 mm, respectively. The ratio of the lateral displacement in the face and the height of the wall was equal to 1.5%. Moreover, the lateral displacements measured in I2 (nonreinforced zone) were negligible (<2 mm).

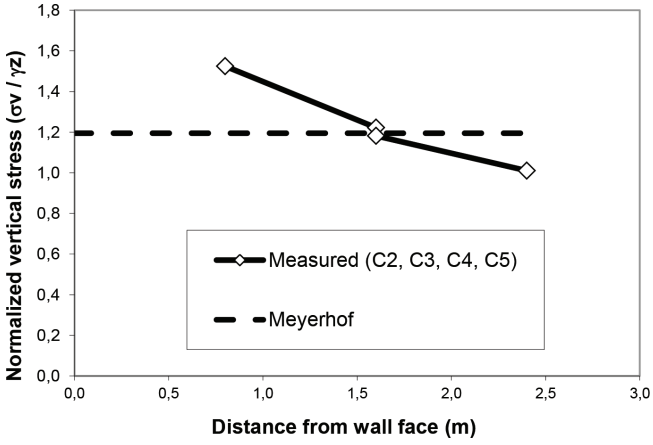

Figure 11. Measured and calculated vertical stress at the base of the wall at the end of construction (third layer).

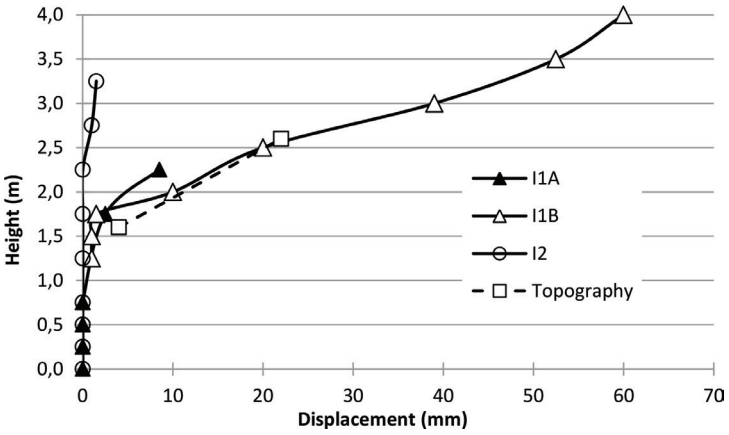

Figure 12. Lateral displacements measured by inclinometers and topographic readings at the end of construction.

2.3.5. Vertical displacements

Vertical displacements were measured during and at the end of construction using magnetic settlement plates (P1–P10; see **Figure 5**). Those plates were positioned both in the reinforced zone and the nonreinforced zone. **Figure 13** presents the vertical displacements at the end of construction; the maximum vertical displacement was equal to 18 mm, recorded by the settlement plate P6. Some plates record values equal to zero or less than 2 mm (P4, P7, P8, and P10). Due to the heavy backfill compaction, most of the vertical displacements have occurred during the wall construction. The heavy compaction induces a kind of a preloading of the soil, and it becomes stiffer, preventing additional vertical deformations during the wall service life [11].

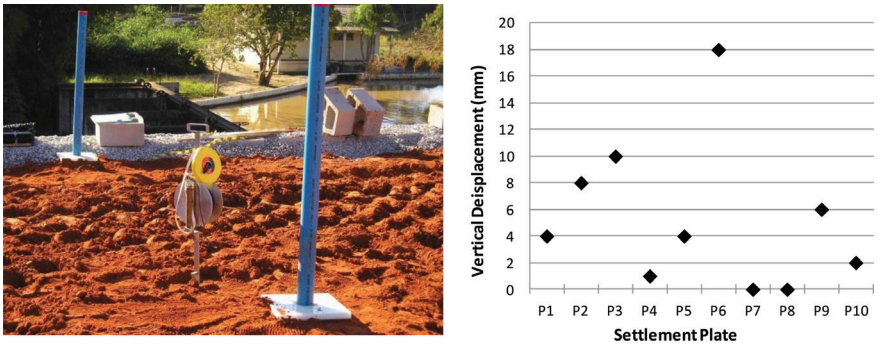

(a) (b)

Figure 13. Magnetic settlement plates: (a) view in the field; (b) results at the end of construction.

3. Comparison of measurements and prediction of tension in reinforcements

The basic concept of internal design includes analysis of failure of reinforcement, i.e., it is to verify if the maximum calculated load in the reinforcement (T_{max}) using appropriated method is lower than the design load of the selected reinforcement (T_d). In addition, verification against pullout failure must be done. The design should provide enough length of the reinforcement in the resistance zone (beyond the potential failure surface) to avoid pullout failure. The design strength T_d is estimated at the end of a given reference time (service life) for a particular installation environment and damage that may occur during installation. T_d can be determined by Eq. (1). In this equation, the terms f_f, f_d, and f_a are reduction factors that are dependent of the type of fabric, the service life, the particular installation environment, and damage that may occur during installation.

$$T_d = \frac{T_{ult}}{f_f \cdot f_d \cdot f_a} \quad (1)$$

where

T_{ult} = ultimate tensile strength, i.e., tensile resistance in short-term resistance obtained from the wide-width tensile strength test (the nominal resistance of the geosynthetic);

f_f = creep reduction factor;

f_d = mechanical damage reduction factor;

f_a = reduction factor for chemical and environmental damages.

Table 5 shows the values of T_d and the reduction factors for the installation conditions and geogrids used in the presented wall (see **Table 3**). The reduction values were evaluated considering that: PET geogrid was used as reinforcement; the design service life is 120 years; the pH of residual lateritic soils is around 5 (installation environment); and low damage during geogrid installation (0.30-m thick backfill layers of fine-grained soil and roller drum Dynapac CA250PD). Moreover, in all reinforcement layers, the values of T_d must be higher than T_{max} considering an appropriated factor of safety (FS ≥ 1.5).

Figure 14 shows comparison of measured and calculated load in reinforcements. The determination of maximum load in the reinforcement layers was done using the analytical method presented by Ehrlich and Mitchell [4]. Through this method, backfill shear resistance,

Geogrid	T_{ult} (kN/m)	f_f	f_d	f_a	T_d (kN/m)
1–3	55	1.67	1.05	1.1	28.5
4–7	35	1.67	1.05	1.1	18.1

Table 5. Reduction factors, T_{ult} and T_d values for the fabrics (geogrids) used in the design of the wall.

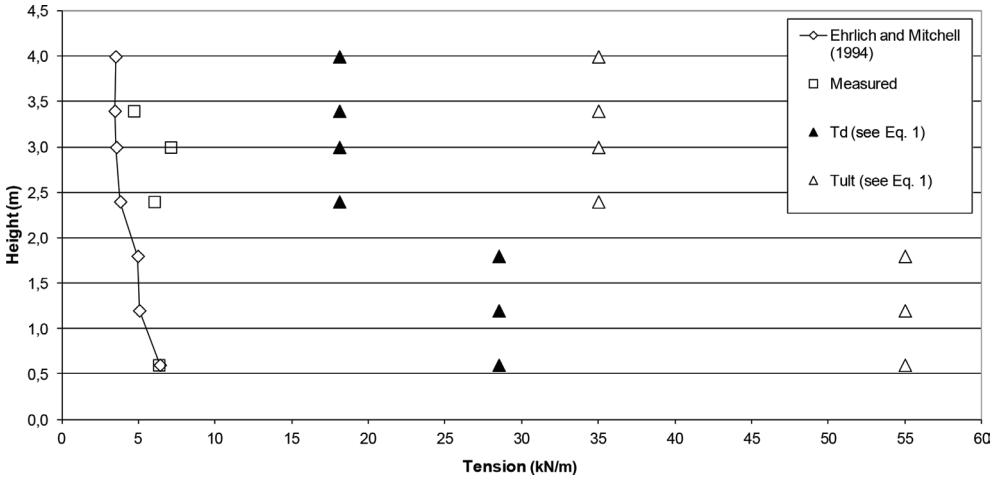

Figure 14. Comparison of T_d and T_{max} measurements and predictions.

reinforcement, and soil stiffness properties are considered, and the backfill compaction stresses are taken explicitly into account. The induced stress due to compaction has the effect of increasing the tension in the reinforcements and the soil cohesion reduced it. In the calculation, the nonconsideration of those factors may lead to poor prediction capability of the real behavior found in the field.

Figure 14 presents that measurements and calculated values of maximum load in the reinforcement (T_{max}) are smaller than T_d. These results also indicate that the predicted values are close to the measured ones, attesting the good performance of the method that was used in the analysis. Additional discussion about measurements and prediction, including determined results using other methods found in the literature, is present in [6].

4. Conclusions

The mechanical behavior of reinforced soil wall built with fabrics (geogrids) is presented based on results of a well-instrumented wall. In this concrete-block-face reinforced wall, tropical fine-grained soils were used as backfill, and two type of fabrics were used as reinforcement. This wall was constructed in 2006 and presents good performance without any structural problem or excessive deformation until nowadays.

Measurements and calculated values of tensions in the reinforcements using an analytical method [4] were compared. Good prediction capability of the used method was verified. In accordance to the good performance of the wall, measurements indicate low vertical and lateral movements, and the mobilized load in the reinforcements was lower than the design load. Measurements also indicate that the block-face supported part of the load that would be carried by the reinforcements.

The fabrics used in the construction were capable to resist the efforts imposed by the structure. The measured mobilized tensions on fabrics (T_{max}) were lower than the design strength (T_d). Considering that T_d is the maximum tension that can act on fabric (T_d is a portion of T_{ult}), it is observed that the wall has safety in terms of internal stability.

Acknowledgements

The authors would like to thank the Brazilian Research Council (CNPq) and HUESKER Synthetics for the support for this work.

Author details

Mario Riccio[1]* and Mauricio Ehrlich[2]

*Address all correspondence to: mvrf1000@gmail.com

1 PEC-UFJF, Federal University of Juiz de Fora, Juiz de Fora, Brazil

2 COPPE-UFRJ, Federal University of Rio de Janeiro, Brazil

References

[1] AASHTO. AASHTO LRFD Bridge Design Specifications. 7th ed. Washington DC; 2014. p. 2150. ISBN: 9781560515920

[2] BSI. BS 8006-1: Code of Practice for Strengthened=Reinforced Soils and Other Fills. London, UK: BSI; 2010

[3] Bathurst RJ, Miyata Y, Nernheim A, Allen AM. Refinement of K-stiffness method for geosynthetic-reinforced soil walls. Geosynthetics International. 2008;**15**(4):269-295. DOI: 10.1680/gein.2008.15.4.269

[4] Ehrlich M, Mitchell JK. Working stress design method for reinforced soil walls. Journal of Geotechnical Engineering, ASCE. 1994;**120**(4):625-645. DOI: 10.1061/(ASCE) 0733-9410(1994)120:4(625)

[5] Ehrlich M, Mirmoradi H. A simplified working stress design method for reinforced soil walls. Géotechnique. 2016;**66**(2):854-863. DOI: 10.1680/jgeot.16.P.010

[6] Riccio M, Ehrlich M, Dias D. Field monitoring and analyses of the response of a block-faced geogrid wall using fine-grained tropical soils. Geotextiles and Geomembranes. 2014;**42**:363-374. DOI: 10.1016/j.geotexmem.2014.01.006

[7] Stuedlein W, Allen T, Holtz R, Christopher B. Assessment of reinforcement strains in very tall mechanically stabilized earth walls. Journal of Geotechnical and Geoenvironmental Engineering, ASCE. 2012;**138**(3):345-456. DOI: 101061/(ASCE)GT.1943-5606.0000586

[8] Mimorardi H, Ehrlich M. Numerical evaluation of the behavior of GRS walls with segmental block facing under working stress conditions. Journal of Geotechnical and Geoenvironmental Engineering. 2015;**141**(3):04014109. DOI: 101061/(ASCE)GT.1943-5606.0001235

[9] Mimorardi H, Ehrlich M. Investigation of the prediction capability of the EM design method under working stress conditions. In: Proceedings of GeoShanghai 2018 International Conference: Geoenvironment and Geohazard. GSIC 2018; Springer, Singapore. pp. 527-536

[10] Ehrlich M, Mimoradi H, Saramago R. Evaluation of the effect of compaction on the behavior of geosynthetic-reinforced soil walls. Geotextiles and Geomembranes. 2012;**34**: 108-115. DOI: 101016/j.geotexmem.2012.05.005

[11] Ehrlich M, Mitchell JK. Working stress design method for reinforced soil walls- clousure. Journal of Geotechnical Engineering, ASCE. 1995;**121**(11):818-821

[12] Mirmoradi SH, Ehrlich M. Modeling of the compaction-induced stress on reinforced soil walls. Geotextiles and Geomembranes. 2015;**43**(1):82-88. DOI: 10.1016/j.geotexmem.2014.11.001

[13] Carvalho PA, Wolle CM, Pedrosa JABA. Reinforced soil embankment using geotextile, an alternative for geotechnical engineering. In: Proceedings from 8th Brazilian Conference on Soil Mechanics and Foundation Engineering; Porto Alegre, Brazil; 1986. pp. 168-178, (in Portuguese)

[14] Ehrlich M, Vianna AJD, Fusaro F. Performance behavior of a geotextile reinforced soil wall. In: Proceedings from 10th Brazilian Conference on Soil Mechanics and Foundation Engineering; Foz do Iguaçu, Brazil; 1994. p. 819e824 (in Portuguese)

[15] Bruno AC, Ehrlich M. Performance of a geotextile reinforced soil wall. In: Proceedings from 2nd Pan-American Symposium on Landslides; Rio de Janeiro, Brazil; 1997. pp. 665-670

[16] Ehrlich M, Delma V, Carvalho P. Performance of two reinforced soil slopes. In: Recent Developments in Soil and Pavement Mechanics. Balkema; 1997. pp. 415-420

[17] Benjamin CVS, Bueno BS, Zornberg JG. Field monitoring evaluation of geotextile-reinforced soil-retaining walls. Geosynthetics International. 2007;**14**(2):100-118. DOI: 10.1680/gein.2007.14.2.100

[18] Brugger PJ, Schmidt CF, Hemsi PS. High height GRW with green wrapped facing. In: Proceedings from REGEO/Geossintéticos; Belo Horizonte, Brazil: CD-ROM (in Portuguese); 2011

[19] Duncan JM, Byrne P, Wong KS. Strength, Stress-Strain and Bulk Modulus Parameters for Finite Element Analyses of Stresses and Movements in Soil Masses. California, USA: University of California, Berkeley; 1980; Report UCB/GT/80-01

[20] Ehrlich M, Becker LB. Reinforced Soil Walls and Slopes, Design and Construction. 1st ed. Boca Raton: CRC Press; 2009. p. 126

[21] Riccio MVF, Ehrlich M. Monitoring of a geogrid reinforced soil wall with segmental block facing. In: Proceedings from Proc. GeoAmericas; Lima, Peru.CD-ROM; 2012

[22] Mirmoradi SH, Ehrlich M. Evaluation of the combined effect of toe resistance and face inclination on the behavior of GRS walls. Geotextiles and Geomembranes. 2016;**44**(3):287-294. DOI: 10.1016/j.geotexmem.2015.12.003

[23] Leshchinsky D, Vahedifard F. Impact of toe resistance in reinforced masonry block walls: Design dilemma. Journal of Geotechnical and Geoenvironmental Engineering, ASCE. 2012;**137**(2):236-240. DOI: 10.1061/(ASCE)GT.1943-5606.0000579

[24] Ehrlich M, Mirmoradi SH. Evaluation of the effects of facing stiffness and toe resistance on the behavior of GRS walls. Geotextiles and Geomembranes. 2013;**40**:28-36. DOI: 10.1016/jgeotexmem.2013.07.012

[25] Meyerhof GG. The bearing capacity of foundations under eccentric and inclined loads. In: Proceedings from 3rd International Conference on Soil Mechanics and Foundation Engineering; Zurich, Switzerland; 1955. pp. 440-445